

BRIEF COMMUNICATION OPEN



Monitoring global climate change using GNSS radio occultation

Hans Gleisner¹✉, Mark A. Ringer² and Sean B. Healy³

The emerging signal of climate change is now clearly evident in Global Navigation Satellite System (GNSS) radio occultation (RO) data, matching predictions made by climate models 15 years ago. The observed RO trends represent well-understood responses to global warming, in particular the widespread cooling of the lower stratosphere and warming of the troposphere. This demonstrates the value of RO measurements for climate monitoring, consistent with their information content and their use in both weather forecasting and atmospheric reanalyses.

npj Climate and Atmospheric Science (2022)5:6; <https://doi.org/10.1038/s41612-022-00229-7>

The GNSS-RO technique is based on measuring the refraction of GNSS radio signals as they propagate on near-horizontal paths through the atmosphere¹. RO instruments on board satellites in low-Earth orbit observe GNSS radio signals rising or setting at the Earth's limb (Fig. 1). A single instrument observes many hundred occultation events per day, quasi-randomly distributed across the Earth and unaffected by clouds and the underlying surface. These data provide a source of observational information with high vertical resolution and long-term stability^{2–4}, extending from near the surface to the upper stratosphere. They are becoming increasingly useful for climate monitoring and climate model testing as the RO measurement time series becomes longer.

During an occultation event a vertical profile of refraction, or “bending”, angles of the GNSS radio signal is measured. The bending angles are converted to a vertical profile of the refractive index, which is followed by retrieval of temperature and pressure profiles (see Methods). Bending angle is the variable closest to the raw measurement and is essentially bias-free up to the upper stratosphere. This property, unique to measurements of the atmosphere, is exploited in numerical weather prediction (NWP)⁵. Most NWP centres now assimilate bending-angle profiles, rather than any of the retrieved geophysical variables, as these can be used without bias correction (referred to as “anchor measurements”). This characteristic also makes them useful for climate reanalyses⁶, and the consistency of the major global temperature reanalyses in the stratosphere has improved since the number of RO measurements increased dramatically in 2006^{7,8}. Combined with the all-weather capability of RO and the long-term stability across successive satellite missions, bending-angle data are clearly well-suited for climate monitoring. We stress that the RO bending angle is a more fundamental quantity than the RO geophysical retrievals (refractive index, temperature, pressure), requiring fewer assumptions and less a priori information, and is therefore suitable when small observational biases throughout the stratosphere is a priority.

Here we use monthly mean, zonally averaged bending-angle data provided by the EUMETSAT RO Meteorology Satellite Application Facility (ROM SAF), and extending from 2002 to the present⁴, to examine atmospheric trends over the last two decades. The trends are computed by ordinary linear regression of monthly mean anomaly time series at each latitude-height grid

point. We show that the bending-angle trends are consistent both with well-understood responses of the UTLS region to long-term global warming^{9–11} and with predictions made with the HadGEM1 climate model almost 15 years ago¹².

The observed trends in bending-angle anomalies as a function of latitude and height (Fig. 2a) correspond to widespread lower-stratospheric cooling over time, which extends across the tropics and sub-tropics and into the mid and high latitudes in the Northern Hemisphere. A consistent pattern is seen in the atmospheric refractivity trends (Fig. 2c), directly reflecting the trends in air density (see Methods), while the associated trends in temperature (Fig. 2d) show tropospheric warming and a transition to stratospheric cooling across a relatively sharp vertical gradient in the tropopause region. We note that the UTLS region, where we find a clear signal of climate change, is also where we find the largest beneficial impacts of RO measurements in operational NWP systems⁵.

The observed bending-angle trends at low- and mid-latitudes (shown in Fig. 2a) are remarkably similar to those predicted in the modelling study of Ringer and Healy [2008]¹² which used the version of the Met Office Hadley Centre climate model (HadGEM1) dating from 2006¹³ and a plausible IPCC emissions scenario for the 21st century. These model results are reproduced in Fig. 2b. The model and observation data sets differ near the poles, consistent with the higher variability at high latitudes. The climate model projections highlighted how the expected atmospheric responses to increased greenhouse gas concentrations—a warming of the upper troposphere and cooling of the lower stratosphere with a sharp gradient at the tropopause; a general upward expansion of the atmosphere which is manifested as an increase of the pressure at fixed altitudes—would lead to well-defined consequences for the distribution of the bending angles. In addition, they suggested that the bending-angle signal in the equatorial lower to middle stratosphere would be clearly identifiable by the 2020s, while that at higher latitudes was more variable and not clearly established until the 2040s.

We also note that not only are the observed bending-angle trends at low- and mid-latitudes structurally very similar to the HadGEM1 model projections but they also have similar magnitudes. For example, the observed trends are around three-quarters of those predicted by the model in the lower stratosphere. The

¹Danish Meteorological Institute (DMI), Copenhagen, Denmark. ²Met Office Hadley Centre, Exeter, UK. ³European Centre for Medium-range Weather Forecasts (ECMWF), Reading, UK. ✉email: hgl@DMI.dk

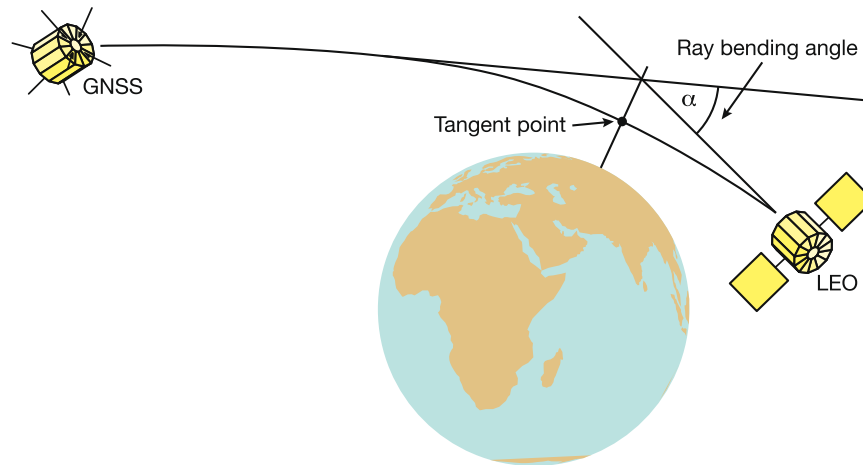


Fig. 1 The radio occultation observation geometry. When the GNSS radio signals pass through the atmosphere they are bent, or refracted, towards the Earth's surface because of the vertical gradient of the refractive index. This causes a time delay that can be measured by the phase shift of the radio signals, in excess of the phase shift expected from the relative velocities between the two satellites. The corresponding refraction angle, or ray bending angle, can be computed from this excess phase. Note that the bending angle has been exaggerated for illustration purposes. It is typically of the order of 1° near the Earth's surface and falls off exponentially with altitude. The time required to sample the radio signal from an altitude of around 100 km to the surface is 1–2 min.

main differences with the model are at high latitudes, in line with the expectation that those trends are likely to be more uncertain.

The time it takes to detect trends depends on the noise characteristics of the time series. Where natural variability is large—due to either unpredictable events, such as volcanic eruptions, or more predictable ones like sudden stratospheric warmings in the polar regions and the Quasi-Biennial Oscillation (QBO) in the equatorial stratosphere—the trend detection times become longer. The observational RO climate data records have been shown to contain accurate information on QBOs¹⁴, and are expected to provide realistic estimates of the natural variability in the low-latitude stratosphere. Based on the HadGEM1 climate model, Ringer and Healy [2008] suggested that climate trends in the tropical stratosphere bending angles would be clearly detected from 11–16 years of data, and demonstrated how the model trends converged towards their final value in accordance with that analysis. Figure 2e shows the evolution of the observed bending-angle trends as the time series becomes longer. After 19 years the trend values have largely converged and become stable, indicating that the current length of the time series is sufficient for trends to be detected with some confidence. Unrealistically low natural variability in climate models may lead to underestimation of the detection times even though the trends themselves are accurately described, a point noted by Ringer and Healy [2008]. Subsequent development of climate models, in particular higher vertical resolution, has led to significant improvements in the representation of variability over time, e.g. in the representation of the QBO¹⁵.

To conclude, analysis of the now 20-year record of GNSS-RO measurements suggests the following: climate trends consistent with our understanding of the response to global warming are clearly identified in the observed monthly mean RO bending angles (Fig. 2a) and in the geophysical variables (Fig. 2c, d) retrieved from the bending angles; these climate signals are seen in regions where the information content of the RO measurements is largest and where the value of RO in both NWP and climate reanalyses is firmly established; the observed bending-angle trends match predictions made with the HadGEM1 climate model a decade and a half ago (Fig. 2b), implying that both the observed signals and models are grounded in robust, well-understood physics. This final point is analogous to that made by Stouffer and Manabe [2017] in relation to projections of surface temperature change made with earlier generations of climate

models¹⁶. It confirms the expected capabilities of RO data expressed two decades ago¹⁷, and suggests that the satellite-derived bending angles provide a valuable observational data source for climate model development and evaluation.

METHODS

Processing of atmospheric profiles

During an occultation event (Fig. 1) the time delay (phase shift) and amplitude of the GNSS radio signal are measured and transformed into a vertical profile of refraction angles, or bending angles, a . Under the assumption of local spherical symmetry around the occultation point, we can use the Abel transform to compute a vertical profile of refractive index, n , from the bending angles

$$\ln n(x) = \frac{1}{\pi} \int_x^\infty \frac{a(a)}{\sqrt{a^2 - x^2}} da \quad (1)$$

where a is the impact parameter and $x = nr$, with r being the radius of a point on the radio signal ray path¹. The microwave refractive index is a function of pressure, p , temperature, T , and water vapour partial pressure, e ,

$$N = (n - 1)10^6 = k_1 \frac{p}{T} + k_2 \frac{e}{T} + k_3 \frac{e}{T^2} \quad (2)$$

where N is referred to as refractivity. For a dry atmosphere, refractivity is directly proportional to air density, and a pressure profile can be retrieved by vertical integration of the refractivity profile under the assumption of hydrostatic equilibrium. The corresponding temperature profile is obtained from an equation of state, e.g. for an ideal gas. This so-called “dry” approximation is a valid assumption in the upper troposphere and throughout the stratosphere¹⁸.

We emphasise that the successive steps in this processing chain involve the use of a priori information. The retrieval of refractivity requires the bending-angle profile in Eq. (1) to be extrapolated to infinity, while hydrostatic integration of a refractivity profile requires an assumption about the pressure at high altitude. Bending angle is the least biased RO variable in the stratosphere, regarded as essentially bias-free, and is the preferred variable for use in NWP⁵ and atmospheric reanalysis⁶. The RO measurements, including the retrieved geophysical variables (refractivity, temperature, pressure), are most precise and accurate at altitudes between 8 and 30 km^{2–4}, in the upper troposphere lower stratosphere (UTLS), where they also have the stability required for climate studies.

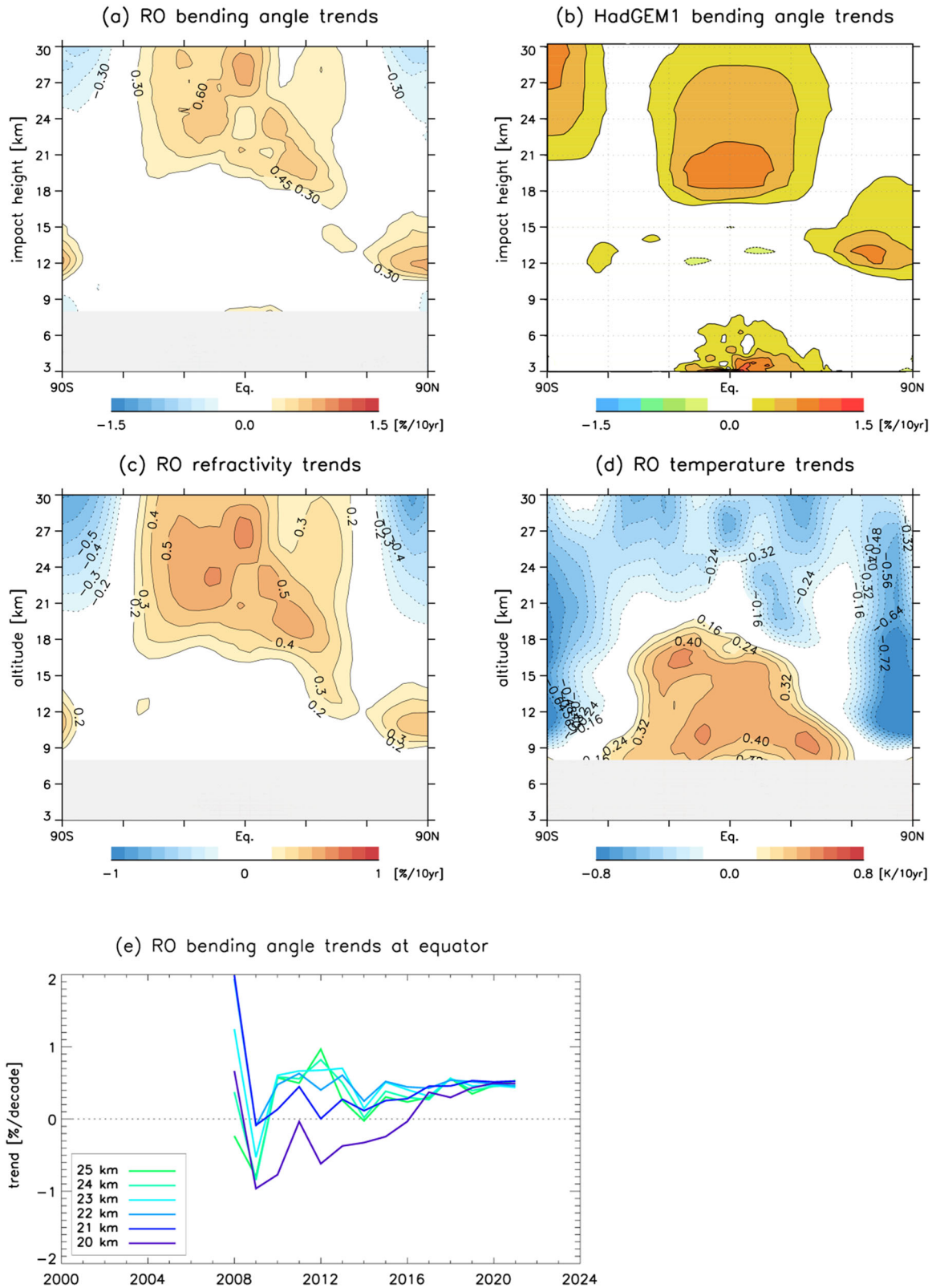


Fig. 2 Long-term trends in radio occultation data and in climate model data. **a** Trends in RO bending-angle anomalies as a function of latitude and height. **b** The corresponding trends in bending-angle anomalies from HadGEM1 climate model integrations under the IPCC A1B scenario, adapted from Fig. 1 in Ringer and Healy [2008]. **c** Trends in refractivity anomalies retrieved from the RO bending angles. **d** The corresponding trends in temperature anomalies. All observed trends are based on data from 2002 to 2020. The bending-angle trends (**a**, **b**) and refractivity trends (**c**) are expressed as percent per decade and the temperature trends (**d**) as kelvin per decade. **e** Evolution of the bending-angle trend estimate in the equatorial (10°S – 10°N) lower stratosphere as the time series becomes longer.

Monthly mean gridded data and anomaly time series

RO data from four satellite missions were combined to form a continuous data record covering 2002–2020⁴. After quality screening and interpolation of the vertical profiles onto an equidistant 200 m height grid, zonally gridded monthly means were computed within 5° latitude bands and calendar months. Estimates of sampling errors were obtained from reanalysis short-term forecast data (by subtraction of true model monthly means from monthly means based on sub-sampled model data) and subsequently subtracted. Finally, anomalies are computed by subtracting a mean seasonal cycle at each latitude and height bin. The trends are computed by ordinary linear regression of the monthly mean anomaly time series at each grid point.

DATA AVAILABILITY

The ROM SAF climate data record v1.0 (https://doi.org/10.15770/EUM_SAF_GRM_0001) and interim climate data record v1 series (https://doi.org/10.15770/EUM_SAF_GRM_0006) were used in this study. The RO data are available at <https://www.romsaf.org>.

Received: 30 April 2021; Accepted: 12 January 2022;

Published online: 03 February 2022

REFERENCES

- Kursinski, E. R., Hajj, G. A., Schofield, J. T., Linfield, R. P. & Hardy, K. R. Observing Earth's atmosphere with radio occultation measurements using the Global Positioning System. *J. Geophys. Res.* **102**, 23429–23465 (1997).
- Steiner, A. K. et al. Quantification of structural uncertainty in climate data records from GPS radio occultation. *Atmos. Chem. Phys.* **13**, 1469–1484 (2013).
- Steiner, A. K. et al. Consistency and structural uncertainty of multi-mission GPS radio occultation records. *Atmos. Meas. Tech.* **13**, 2547–2575 (2020).
- Gleisner, H., Lauritsen, K. B., Nielsen, J. K. & Syndergaard, S. Evaluation of the 15-year ROM SAF monthly mean GPS radio occultation climate data record. *Atmos. Meas. Tech.* **13**, 3081–3098 (2020).
- Bauer, P., Radnóti, G., Healy, S. & Cardinali, C. GNSS radio occultation constellation observing system experiments. *Mon. Weather Rev.* **142**, 555–572 (2014).
- Hersbach, H. et al. The ERA5 global reanalysis. *Q. J. R. Meteorol. Soc.* **146**, 1999–2049 (2020).
- Long, C. S., Fujiwara, M., Davis, S., Mitchell, D. M. & Wright, C. J. Climatology and interannual variability of dynamic variables in multiple reanalyses evaluated by the SPARC Reanalysis Intercomparison Project (S-RIP). *Atmos. Chem. Phys.* **17**, 14593–14629 (2017).
- Ho, S.-P. et al. The COSMIC/FORMOSAT-3 radio occultation mission after 12 years: Accomplishments, remaining challenges, and potential impacts of COSMIC-2. *Bull. Am. Meteorol. Soc.* **101**, E1107–E1136 (2020).
- Santer, B. D. et al. Tropospheric warming over the past two decades. *Sci. Rep.* **7**, 2336–2342 (2017).
- Maycock, A. C. et al. Revisiting the mystery of recent stratospheric temperature trends. *Geophys. Res. Lett.* **45**, 9919–9933 (2018).
- Steiner, A. K. et al. Observed temperature changes in the troposphere and stratosphere from 1979 to 2018. *J. Clim.* **33**, 8165–8194 (2020).
- Ringer, M. A. & Healy, S. B. Monitoring twenty-first century climate using GPS radio occultation bending angles. *Geophys. Res. Lett.* **35**, L05708 (2008).
- Johns, T. C. et al. The new Hadley Centre climate model (HadGEM): evaluation of coupled simulations. *J. Clim.* **19**, 1327–1353 (2006).
- Healy, S. B., Polichtchouk, I. & Horányi, A. Monthly and zonally averaged zonal wind information in the equatorial stratosphere provided by GNSS radio occultation. *Q. J. R. Meteorol. Soc.* **146**, 3612–3621 (2020).
- Butchart, N. et al. QBO changes in CMIP6 climate projections. *Geophys. Res. Lett.* **47**, e2019GL086903 (2020).
- Stouffer, R. J. & Manabe, S. Assessing temperature pattern projections made in 1989. *Nat. Clim. Change* **7**, 163–165 (2017).
- Steiner, A. K. et al. GNSS occultation sounding for climate monitoring. *Phys. Chem. Earth A* **26**, 113–124 (2001).
- Danzer, J., Foelsche, U., Scherlin-Pirscher, B. & Schwärz, M. Influence of changes in humidity on dry temperature in GPS RO climatologies. *Atmos. Meas. Tech.* **7**, 2883–2896 (2014).

ACKNOWLEDGEMENTS

The radio occultation data were provided by the Radio Occultation Meteorology Satellite Application Facility (ROM SAF), which is a decentralised RO processing center under EUMETSAT. H.G. and S.H. were supported by the ROM SAF. M.R. was supported by the Met Office Hadley Centre Climate Programme funded by BEIS and Defra.

AUTHOR CONTRIBUTIONS

The study was designed and carried out as a team effort including contributions from all three authors. H.G. performed the main analysis, generated the figures, and prepared the manuscript with contributions from M.R. and S.H.

COMPETING INTERESTS

The authors declare no competing interests.

ADDITIONAL INFORMATION

Correspondence and requests for materials should be addressed to Hans Gleisner.

Reprints and permission information is available at <http://www.nature.com/reprints>

Publisher's note Springer Nature remains neutral with regard to jurisdictional claims in published maps and institutional affiliations.



Open Access This article is licensed under a Creative Commons Attribution 4.0 International License, which permits use, sharing, adaptation, distribution and reproduction in any medium or format, as long as you give appropriate credit to the original author(s) and the source, provide a link to the Creative Commons license, and indicate if changes were made. The images or other third party material in this article are included in the article's Creative Commons license, unless indicated otherwise in a credit line to the material. If material is not included in the article's Creative Commons license and your intended use is not permitted by statutory regulation or exceeds the permitted use, you will need to obtain permission directly from the copyright holder. To view a copy of this license, visit <http://creativecommons.org/licenses/by/4.0/>.

© The Author(s) 2022